

DYNAMIC PROPERTIES OF THE SHOULDER COMPLEX BONES

Sudipto, Mukherjee
Anoop, Chawla,
Saurabh, Borouah
Debashish, Sahoo
Mike W. J. Arun

Department of Mechanical Engineering, IIT Delhi
India

Girish, Sharma
Parthiv Shah

Christophe Ageorges
Mercedes Benz R&D India
India
Paper Number 11-0428

ABSTRACT

This paper reports a characterization of stress-strain response of the humerus, clavicle and scapula through impact studies followed by property estimation. For the humerus, the modulus obtained for quasi-static tests varies between 0.4 to 18 GPa while the modulus obtained from the drop height of 0.5m varies from 0.7 to 40.5 GPa, that obtained from a drop height of 1m varies from 0.8 to 40.95 GPa and that from the 1.5m drop tests varies from 1.8 to 53 GPa. The increase in modulus with strain rate is consistent with earlier studies including McElahney [[5]].

INTRODUCTION

Safety measures have traditionally been evaluated by full-scale crash testing. The high cost and that it can be conducted only after a prototype is available has been a barrier in investigating alternatives for limiting injuries. Computer simulations are cost effective as compared to full-scale crash tests, and also provide a great deal of information that is frequently unavailable from full-scale crash testing. Unlike full-scale crash tests that normally yield data for only predetermined points where sensors have been mounted, computer simulations can be used to track all areas where a design needs additional reinforcement or areas where a component has excess capacity. For example, finite element modeling provides designers with an accurate picture of the stress distributions in critical components of a safety device throughout the impact event. Sicking and Mak [[6]] note that After a computer simulation has been developed and successfully validated against full-

scale crash tests, the cost associated with conducting parametric studies to investigate the effects of installation details, impact conditions, road furniture, and vehicle characteristics is relatively inexpensive.

Computer simulations of vehicle collisions have improved significantly over the past few years. With advances in computer technology and non-linear finite element (FE) codes, full scale models and simulations of sophisticated phenomena like in biological systems are becoming ever more possible. Finite element crash simulations have been primarily focused on the vehicle models and their crash characteristics. Recently, refined FE models of airbags and dummies have been added to the simulations. This allows assessment of occupant injury and restraint system performance. Specifically, a well-developed human body model helps in understanding injury mechanisms and also helps to know the effect of modifications made to vehicles.

Efficient human body model development requires detailed modeling of the geometry of the human body and extensive tissue and bone properties beyond those already available in literature, such as dynamic properties of bones. Mechanical properties of human shoulder bones at strain rates expected in automotive related crashes are reported here. The outboard shoulder is in close proximity to the side door. Shoulder bones characteristics are hence critical in analyzing side impact crashes. As shown in Table 1, the percentage of casualties with AIS (Abbreviated Injury Scale) 3+ injuries to Upper extremities are 12.1 % Holt and Vassey [[4]] to 14.3 % in Dalmotas

[[1]], highlighting the large incidence in the Upper extremities.

Table 1. Percent of three point belted casualties with AIS >=3 in side impacts

BODY REGION	Percentage of injuries with AIS>=3	
	HOLT and VASSEY (1977)	DALMOTAS (1983)
Head/face	46.6	48
Neck	1.7	7.1
Shoulder/chest	48.3	40.8
Pelvis	24.1	13.3
Abdomen	10.3	11.2
Upper extremities	12.1	14.3
Back	0	1

Attempts have been made earlier to study bone properties at high strain rates, often using Split Hopkinson Pressure Bars. Shima et al. [[8]] characterized the dynamic compressive mechanical properties of cancellous bone from the human cervical spine using SHPB. The static and dynamic compressive responses of cancellous bone specimens from the human cervical spine were studied.

Ferreira et al. [[2]] characterized the mechanical properties of bovine cortical bone at high strain rate using SHPB. The study evidenced that bone is a highly heterogeneous structure and scattering of results is significant. It was observed that for an increase of strain rate the resistance properties increased and stiffness properties decreased. Westhuizen et al. [[7]] characterized the strain rate dependent mechanical properties of bovine bone in axial compression by quasi-static and dynamic tests.

Human cadavers (right and left shoulder) in age group 40 — 60 yrs have been tested. Cadaveric bone specimens were tested in three point bending with impact speeds up to 20 kmph. Piezoelectric impactor-force sensor data was acquired in excess of 400 KHz through a digital oscilloscope. A strain gauge mounted at the point opposite to point of impact was used to measure longitudinal strain data. A

REDLAKE MotionXtra HG-LE was used to record displacements at points of interest and locate the time of visible crack initiation at a frame rate of 30,000 frames/s.

Using pre-impact CT images, FE meshes were developed for each individual bone, and material density was estimated using Materialise MIMICS software. The spectrum of material density is clustered into groups, and elastic-plastic properties are initially assigned to each group on the basis of the CT grey values. Impact simulation in LS-DYNA were used to estimate material properties. The region dependant parameters for Cowper Symonds material model for bones are then optimized to match the experimental results. Further, a roadmap to building accurate bone models, through CT scans and assignment of material properties based on grey values to account for nonhomogeneity of bones has been investigated.

In this paper, we will describe the results of the test done on the humerus. The optimized material properties for each bone that resulted in the best fit will be presented as the final result.

The Quasi-Static Test Setup

Three point bending tests with the impactor moving at constant velocity has been used. Figure 1 shows the schematic arrangement for the static three point bending set up.

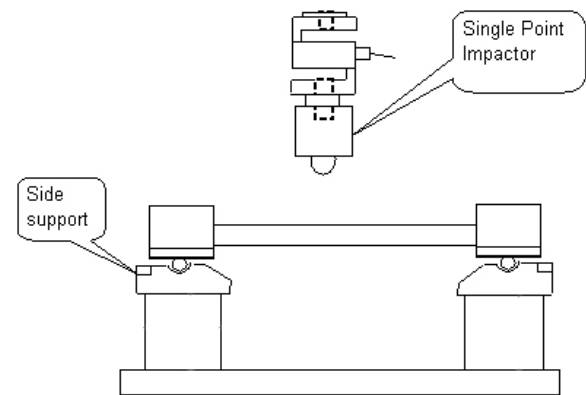


Figure 1. A schematic of the three Point Bending Setup

Figure 2 shows the pre-loading setup for the humerus. The ends are potted using bone cement and

a jig designed especially to maintain the desired alignment during the potting process.

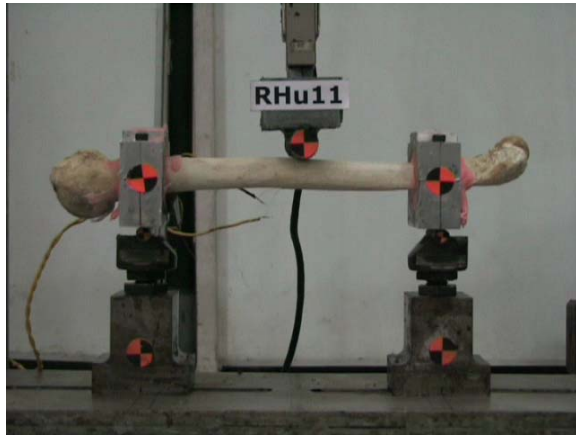


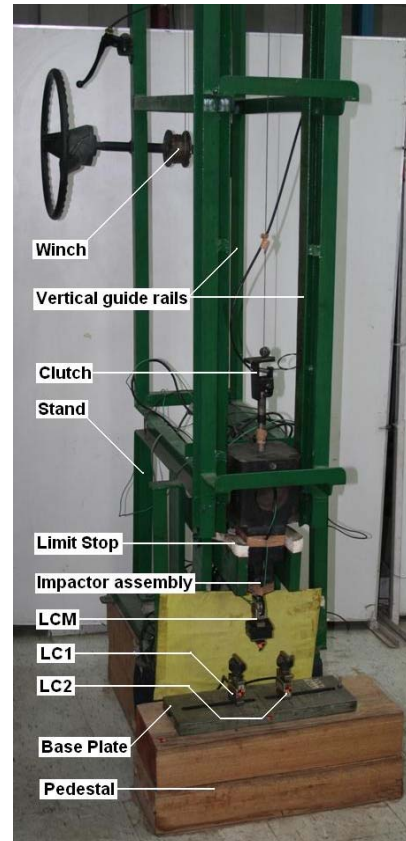
Figure 2. Initial setup of the quasi-static loading on the humerus

The Dynamic Test Setup

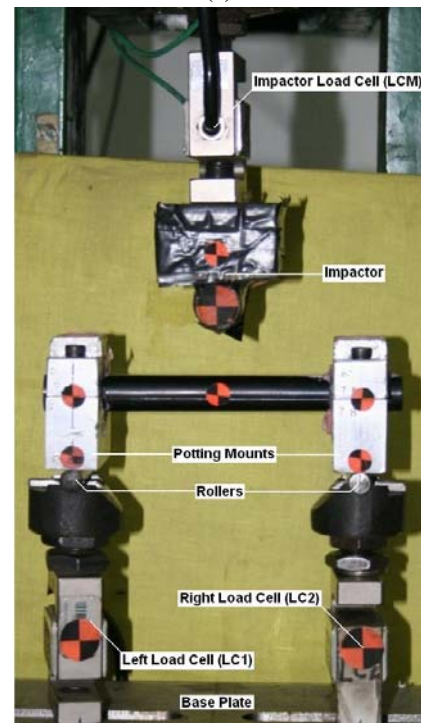
The freefall impactor rig, shown in Figure 3, comprises of an impactor of mass 30.5kg constrained to move between two vertical rails. A cable winch is used to raise the mass to desired height and a sprocket and cowl mechanism is used to hold and release the impactor. The drop height can be set to a maximum of 2m. A load cell in line with the impactor is used to record the impactor force and foam padding is used to arrest the impactor at the end of the stroke to protect the instrumentation. The specimen is positioned so that the bone fractures before the falling impactor comes in contact with the arresting foam.

The base plate, shown in Figure 3, supports the specimen through load cells. The specimen, set in the potting mounts, rests on these rollers mounted on top of the load cells to achieve simply supported boundary conditions.

The average mass of the humerus bones was 204.6 gms, that of the clavicle bones was 30.4 gms and that of the scapula bones was 86.55 gms. For testing the scapula which is not by structure amenable to bending tests, thin strips suitable for bending tests were extracted by milling. These bones were scanned using commercially available CT scanner and then tested.



(a)



(b)

Figure 3. Freefall rig and base plate with supports (a) Full view (b) Close-up of Base Plate and mounts

Table 2. Test matrix

Type of test	Humerus	Clavicle	Scapula (spine)	Scapula (lateral border)
Quasi-static	4	4	5	5
0.5m drop	5	6	5	5
1.0m drop	5	6	5	5
1.5m drop	8	8	5	5
Total	22	24	20	20

Results of testing on Humerus

The quasi static response is presented in **Figure 4**. Four tests and the average of the tests with the $\pm 1\sigma$ band are shown. Dispersion of the stiffness and the failure point between specimens is large. The average stiffness has been projected to the largest displacement seen by the humerus to failure. The bones with higher stiffness have progressively higher force to failure but lower displacement to failure. This has not been reported by earlier researchers like Schriber [[7]]. Though the increase in failure force with increase of stiffness is consistent in the scapula and clavicle tests, the phenomenon of increased displacement to failure with increasing compliance is not observed in the clavicle or scapula tests.

Tests were conducted on four specimens at a drop height of 0.5 m, four specimens at a drop height of 1.0 m and six specimens at a drop height of 1.5 m. The maximum strain rate achieved at a drop height of 1.5m is about 33/s. An average response was defined at each drop height with a spread. The point of failure was identified post-facto based on the high speed camera data and the earliest failure for a particular height was used to determine the time to which the averaging was done. The fracture point was all occasions after the first peak though this is not obvious from the average data for 1.5 m drop. It is seen that for larger drop heights, the peak forces are higher and the failure occurs earlier. It may be pointed out that the average response is not indicative of probable bone response for that drop height, but

the probable bone response at that drop height before crack initiation.

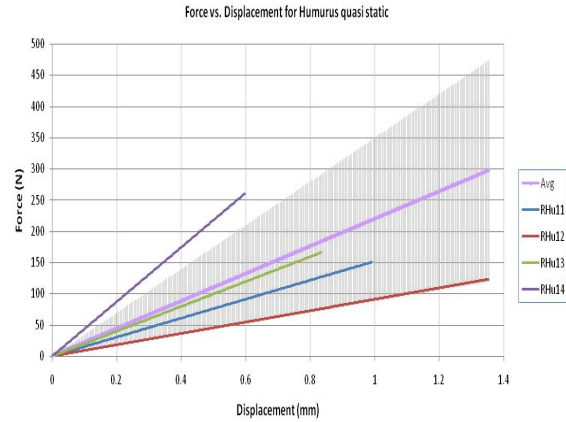


Figure 4. Force vs displacement response for humerus in three point bending.

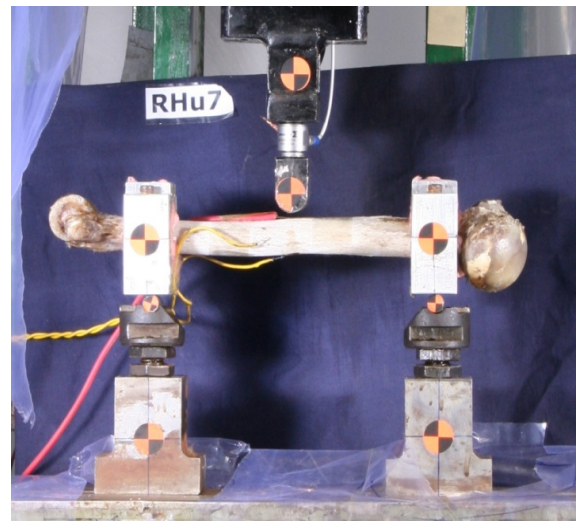


Figure 5. Initial setup of the impact test on the humerus

Figure 5 shows the pre-impact setup for the humerus. In dynamic tests, the mass and moment of inertia properties of the end fixation devices modify the response. These have hence been engineered to leave as small a footprint as possible and have been accurately estimated so that they can be reproduced in the simulations.

Finite element modelling and property extraction

The CT scan data of the bone with the response closest to the average curve obtained was used to

develop a bone model. The loading setup was modeled to mimic the tests in quasi-static as well as impact tests. The setup is shown in Figure 7 below.

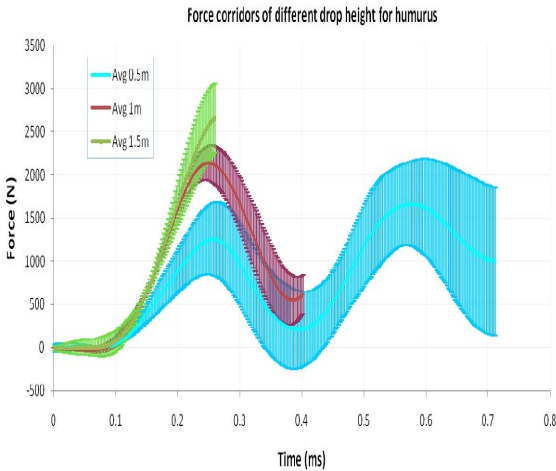


Figure 6 Force corridors for tests done with different drop heights on the humerus

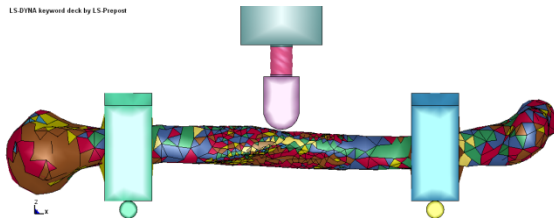


Figure 7. Typical FE model for drop test

The bone models are made of approximately 8500 linear tetrahedral elements made from about 2500 nodes. In order to decide the mesh size a convergence analysis was done by varying the mesh size in various regions of the bone. The bone FE model was finalized with two zones of different mesh density. Elements in mid-diaphysis region have an edge length of approximately 3.5 mm. This fine element region extends to 25mm on either sides of the point of impact. This is done to increase the accuracy of Hertzian contact stress approximation. The rest of the bone is meshed with elements whose edge lengths are approximately 7 mm. In the mesh, the minimum warpage was 5 and the minimum Jacobian was 0.7. Only 1% of the total elements had an aspect ratio more than 5. The average run time of a simulation was approximately 90 seconds when solved using 4

CPUs which clocks data at the rate of 2.33 GHz on a Core 2 Quad processor with 4Gb RAM.

Relationships between CT Hounsfield number, apparent density and elastic modulus were used to assign an *initial* density-dependent modulus for each tetrahedral element [[2]] in ten groups. The net mass of the bone was compared with the measured mass and if needed (variation was usually less than 5%) the density was scaled linearly to match the mass.

The dynamic tests were simulated in LS Dyna and the static tests were simulated in Abaqus. The RMS between the two responses was taken to be the objective function to be minimized by tuning the stiffness. The mapping between the Hounsfield number and modulus is taken to be bilinear with the transition occurring at Hounsfield number of 600 based on a histogram analysis. The parameters of the linear relationship along with yield strain and the maximum plastic strain were altered in the GA run in order to match the simulation response with the average experimental response. In addition, the C & P parameters in the Cowper Symmond's Model were altered in order to capture the shift in the yield stress with strain rate. This was seen to affect only a small set of elements near the point of impact. The optimized responses are shown alongside the average values in Figure 8, Figure 9, Figure 10 and Figure 11 respectively.

The correlations obtained through simulations are listed in Table 3 and have a average fit of 0.897. The quasi static tests consistently have very high fits and the 1.5 m humerus drop has fits of 0.684, which could be said not to be strongly correlated. The match between simulation and experiment for the lateral border of the scapula is not as strong as the rest of the tests. This could be due to problems in idealizing the boundary conditions of the test in the simulation.

Table 4 summarises the estimated properties for the humerus. The modulus obtained for quasi-static tests varies between 0.4 to 18 GPa while the modulus obtained from the drop height of 0.5m varies from 0.7 to 40.5 GPa, that obtained from a drop height of 1m varies from 0.8 to 40.95 GPa and that from the 1.5m drop tests varies from 1.8 to 53 GPa. The increase in modulus with strain rate is consistent with earlier studies including McElahney [[5]].

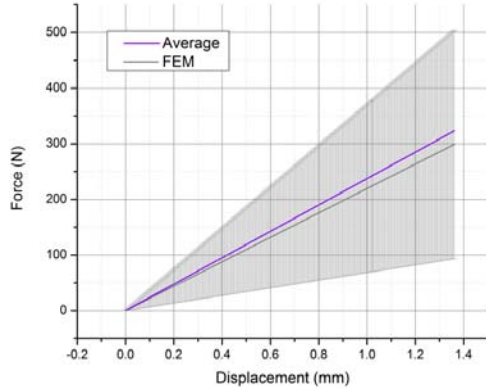


Figure 8 The average experimental and the FEM response for quasi-static test.

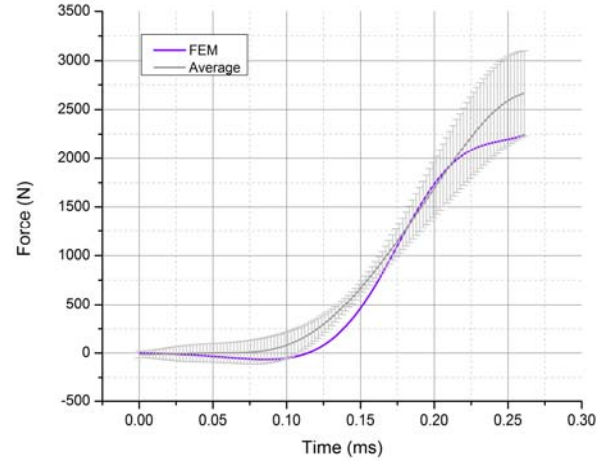


Figure 11. The average experimental and the FEM response for 1.5mtr drop height.

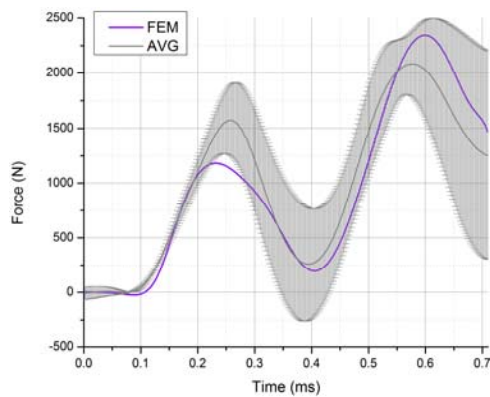


Figure 9 The average experimental and the FEM response for 0.5mtr drop height.

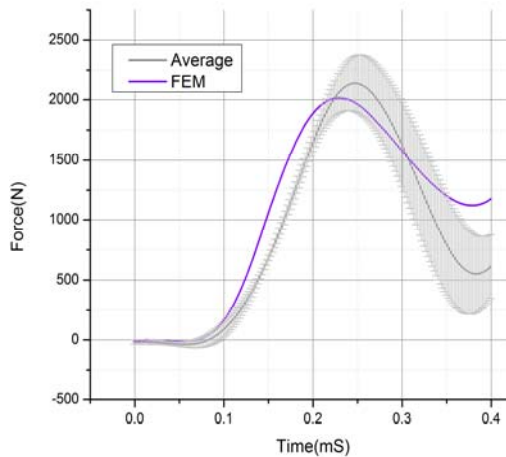


Figure 10. The average experimental and the FEM response for 1 m drop height.

Table 3 Correlations against average experimental value

Humerus 0.5 m drop	0.85752
Humerus 1.0 m drop	0.90481
Humerus 1.5 m drop	0.68421
Humerus quasi-static	0.99963
Clavicle 0.5 m drop	0.94860
Clavicle 1.0 m drop	0.8011
Clavicle 1.5 m drop	0.92337
Clavicle quasi-static	0.99921
Scapula 0.5 m drop	0.99892
Scapula 1.0 m drop	0.99537
Scapula 1.5 m drop	0.70772
Scapula quasi-static	0.99949
Scapula(lat border) 0.5 m drop	0.68553
Scapula(lat border) 1.0 m drop	0.99952
Scapula(lat border) 1.5 m drop	0.85877
Scapula(lat border) quasi-static	0.99952

The response for clavicle and the corresponding estimates of properties have not been listed here for brevity. There are some different trends observed for the scapula which have been listed in the conclusion.

CONCLUSION

A procedure and instrumentation has been established to estimate region based bone properties that reproduce dynamic impact in FE based simulations.

For the same material densities, the modulus for the scapula is much lower than that for the humerus and

the clavicle. For the spine of the scapula, the modulus under dynamic conditions is lower than that under static conditions which is unexpected. It is also noted that in the dynamic tests, the spine of the scapula has a very different failure mode which seems to be similar to a shear failure. This could be resulting from the variance between the microstructure of the scapula and that of the other bones.

Table 4. Estimated modulus and yield stress

		Materials										
		Cancellous			Cortical							
		1	2	3	4	5	6	7	8	9	10	
		Density	132	394	657	918	1181	1443	1705	1968	2230	2492
$\dot{\epsilon}_{TK}$	Hounsfield	1 to 200	399 to 600	871 to 1142	1413 to 1684	1955 to 2226	2500					
	No	200 to 399	600 to 871	1142 to 1413	1684 to 1955	2226 to 2500						
0	ϵ_y 1.8	Young's Modulus (Gpa)	0.413	2.98	5.55	5.55	7.61	9.69	11.76	13.82	15.9	17.96
	ϵ_{pf} 0	Yield Stress (Mpa)	7.44	53.7	100.1	100.1	137.1	174.5	211.68	248.89	286.24	323.5
13.5	ϵ_y 1.2	Young's Modulus (Gpa)	0.7	2.4	4.06	4.06	10.1	16.2	22.3	28.3	34.4	40.5
	ϵ_{pf} 0.9	Yield Stress (Mpa)	8.91	28.8	48.77	48.77	121.3	194.4	267.2	340	413.12	486
20.5	ϵ_y 0.51	Young's Modulus (Gpa)	0.807	3.76	6.729	6.729	12.41	18.13	23.83	29.53	35.26	40.95
	ϵ_{pf} 0.92	Yield Stress (Mpa)	4.11	19.2	34.31	34.31	63.28	92.47	121.54	150.62	179.8	208.9
33	ϵ_y 1.59	Young's Modulus (Gpa)	1.8	6.2	10.6	10.6	17.6	24.7	31.7	38.8	45.9	53.01
	ϵ_{pf} 1.05	Yield Stress (Mpa)	29.31	98.8	168.6	168.6	280.5	393.3	505.56	617.87	730.61	842.9

It is our understanding that though the initiation of the fracture is predicted accurately, the propagation is not predicted accurately by the current method. This needs further refinement. The study is not extensive enough to characterize the full spectrum of crash victims. More tests are planned in the near future to normalize the specimen to specimen variation in the samples and evolve age and gender trends.

The process of optimizing the distribution of bone properties has been limited by the computing resources. A larger number of clusters than currently used could in principle be considered, leading to better fits. Similarly, instead of averaging the response, fitting the properties to individual geometry and estimating an average of properties may be

considered as an alternative given more computational and manpower resources.

REFERENCES

- [1] Dalmotas, D.J., (1983), Injury mechanisms to occupants restrained by three point seat belts in side impact, SAE transactions, 92(2), 2.328-2.354, SAE paper 830462, 1983.
- [2] Dalstra, M., Huiskes, R., Odgaard, A., and van Erning, L., 1993, "Mechanical and Textural Properties of Pelvic Trabecular Bone," J Biomech, 26, pp. 523-35.
- [3] Ferreira F, Vaz MA, Simoes JA, (2005), "Mechanical properties of bovine cortical bone at high strain rate", Materials Characterization, 2005.
- [4] Holt, B.W. & Vazey, B.A, (1977), In depth study of seriously injured seat belt wearers, Report number 1/77, Traffic Accident Research unit, Department of motor transport, 1977.
- [5] McElhaney J.H. (1966) Dynamic response of bone and muscle tissue. Journal of Applied Physiology 21, 1231-1236
- [6] Sicking, D.L and K.K. Mak, Improving Roadside Safety by Computer Simulation, Transportation in the New Millennium, Transportation Research Board, Washington, D.C., January 2000
- [7] Schreiber P., Crandall J., Micek T., Hurwitz S., Nusholtz G. S., "Static and Dynamic bending strength of the leg", IRCOBI Conference - Hannover, September 1997
- [8] Shima V.P.W., Yanga L.M., Liua J.F., Leeb V.S., (2005), "Characterisation of the dynamic compressive mechanical properties of cancellous bone from the human cervical spine", International Journal of Impact Engineering, Volume 32, Pages 525-540, 2005.
- [9] Westhuizen V.D., Cloete T.J., Kok S., Nurick G.N., (2007), "Strain rate dependent mechanical properties of bovine bone in axial compression", IRCOBI Conference, 2007.